Journal of the Serbian Chemical Society
JSCS-info@shd.org.rs • www.shd.org.rs/JSCS
J. Serb. Chem. Soc. 78 (7) 973–986 (2013) UDC 544.2+544.15:544.174.21.3+544.354–128
JSCS–4474 *Original scientific paper*

Ab initio study of vibronic transitions between $X^2\Pi$ and $1^2\Sigma^+$ electronic states of HCP^+

LJILJANA STOJANOVIĆ*#

Faculty of Physical Chemistry, Studentski Trg 12, 11158 Belgrade, Serbia

(Received 15 November, revised 25 November 2012)

Abstract: The ground and low-lying excited doublet electronic states of the HCP^+ were studied by means of the multireference configuration interaction method. The vibronic energy levels of the $X^2\Pi$ state of Σ, Π, Δ, and Φ symmetry, up to the 2500 cm^{-1}, have been calculated variationally, employing previously developed *ab initio* methods that take into account vibronic and spin–orbit interactions. The vibronic wave functions were used to estimate transition moments between vibronic energy levels of the $X^2\Pi$ and $1^2\Sigma^+$ electronic states. The results were compared to available experimental and theoretical data.

Keywords: excited states; Renner–Teller effect; phosphaethyne cation.

INTRODUCTION

The HCP^+ was detected for the first time in a photoelectron spectroscopy experiment on the HCP molecule, when the CP stretching progressions between the ground $X^2\Pi$ and the first excited $1^2\Sigma^+$ state were observed.[1] King *et al*. later recorded electron-impact $1^2\Sigma^+ \rightarrow X^2\Pi$ emission spectra. In their first study,[2] short progressions in the CP stretching vibrations were reported, and the ground state spin–orbit coupling constant and the CP stretching frequency were derived from the spectrum. In a subsequent study,[3] bands of the high-resolution emission spectrum were analyzed and rotational constants of the ground and the first excited state, as well as an improved value of the spin–orbit coupling constant, were derived. Finally, in the latest study,[4] the authors reported the $1^2\Sigma^+ \rightarrow X^2\Pi$ emission spectrum with resolved transitions to $\nu_2'' = 1$ and 2 bending vibrational levels. They were able for the first time to analyze vibronic, spin–orbit, and Fermi resonance structures of the ground state. In the latest study[5] of this ion by Clouthier *et al*., the laser-induced fluorescence (LIF) spectrum between first two states involving all vibrational modes was recorded and a set of vibrational cons-

* Correspondence, E-mail: stojanovicmljiljana@gmail.com
# Serbian Chemical Society member.
doi: 10.2298/JSC121115128S

tants and ground and excited state geometric parameters were derived from the spectrum.

The HCP^+ has also been the subject of several theoretical studies. Initially, they were mainly concerned with the geometries and properties of the potential energy surfaces of the ground and the first excited state.[6–8] Karna and Grein performed the first systematic study of the excited states.[9] They optimized, using the multireference configuration interaction method, the geometries and calculated the vertical excitation energies and stretching frequencies of the nine lowest-lying doublet and quartet electronic states. Later, Temelso *et al*. studied the ground and the first excited state using coupled cluster methods with different basis sets.[10]

The vibronic structure of the $X^2\Pi$ state of HCP^+ was investigated theoretically in two thorough studies. In the first of them, Tarroni *et al*. calculated the MRCI potential energy surfaces of the ground state components and employed a full-dimensional vibrational treatment to calculate the spin–rovibronic energy levels of the ground state employing the Handy–Carter Hamiltonian as the kinetic energy operator.[11] They performed detailed analysis of the Fermi resonance between the bending (v_2) and CP stretching modes (v_3), and concluded that the used effective model Hamiltonian that describes a Fermi interaction was inapplicable when the bending and CP stretching modes are multiply excited (v_2 + + $2v_3$ > 3). The obtained results well reproduced the experimental findings, except that in some cases the ordering of the levels was different from the experimentally derived one.

Clouthier *et al*. also performed a Renner–Teller analysis of the ground state vibrational energy levels.[5] They were able to fit the majority of the levels up to 4500 cm^{-1} (with the exception of several levels) using their previously developed model that includes vibronic, spin–orbit, and Fermi resonance interactions.

In the present study, computation of the bending potential curves of the ground and the nine lowest-lying doublet electronic states of HCP^+ was performed. The obtained bending potential energy curves of the $X^2\Pi$ state were employed in the calculation of the vibronic energy levels using previously developed variational methods with Hamiltonians that incorporate terms describing vibronic and spin–orbit coupling. Finally, the vibronic transition moments between the $X^2\Pi$ and $1^2\Sigma^+$ states were computed employing calculated vibronic wave functions and electronic dipole transition moments.

COMPUTATIONAL AND THEORETICAL METHODS

Electronic ab initio *methods*

The ground and lowest-lying doublet electronic states of the linear HCP^+ were studied by means of the internally contracted MRCI method[12] with a state average complete active space self-consistent field (SA-CASSCF)[13] reference wave function using the Dunning aug-cc-pVTZ basis[14]. The full valence CASSCF computations were performed, *i.e*., the configuration

state functions were formed by distribution of all nine valence electrons within the active space composed of eight orbitals in the $C_{\infty v}$ symmetry group - (5–9)σ and (2–4)π (in the C_{2v} subgroup, it is composed of 11 orbitals - (5–9)a_1, (2–4)b_1, and (2–4)b_2). All computations were performed using the MOLPRO program package.[15]

The geometries of the ground $X^2\Pi$ and $1^2\Sigma^+$ states were optimized at the MRCI level of theory with CASSCF reference functions. In the case of the $X^2\Pi$ state, the reference function was obtained by averaging with equal weights both state components (1^2B_1 and 1^2B_2), whereas the 1^2A_1 CASSCF wave function was used as the reference for the geometry optimization of the $1^2\Sigma^+$ state.

The vertical excitation energies from the ground to the nine lowest-lying doublet states and the bending potential curves of all studied states were computed at the MRCI-optimized bond lengths of the $X^2\Pi$ state within the C_s symmetry group using the MRCI/FV-SA-CASSCF method by averaging with equal weights all the states. The electronic transition moments between the ground and excited CASSCF electronic states were computed as functions of the bending coordinate at the MRCI bond lengths of the ground state.

The spin–orbit coupling constant of the $X^2\Pi$ state was also computed at its MRCI optimized geometry as the difference between the energies of the two spin components obtained by diagonalization of the sum of the Breit–Pauli operator and the electronic operator in the basis of the MRCI components of the state.

In addition, the harmonic vibration frequencies of all three vibrational modes in the $X^2\Pi$ and $1^2\Sigma^+$ states were computed.

Vibronic ab initio *methods*

The Hamiltonian used in this study included operators describing electronic motion, bending vibrations, rotation around axis of the smallest moment of inertia (*z*-axis), and spin–orbit interaction in its phenomenological form ($A_{SO}\hat{L}_z\hat{S}_z$):[16]

$$\hat{H} = \hat{H}_e + \hat{T}_b + \hat{T}_r^z + \hat{H}_{SO}. \quad (1)$$

This model neglects possible couplings between the bending and stretching modes and rotations around axes perpendicular to the axis of the smallest moment of inertia, although Fermi resonance between the CP stretching and bending mode was previously detected.[4] The general form of the kinetic energy operator for bending vibrations and rotation about the z-axis in atomic units is:

$$\hat{T}_b + \hat{T}_r^z = -\frac{1}{2}\left(T_1(\rho)\frac{\partial^2}{\partial\rho^2} + T_2(\rho)\frac{\partial}{\partial\rho} + T_0(\rho) \right) - A(\rho)\frac{\partial^2}{\partial\varphi^2} \quad (2)$$

where ρ is the angle supplementary to the instantaneous bond angle θ, φ is the angle between the molecular plane and the space-fixed plane, which is chosen such that it contains the axis that corresponds to the smallest moment of inertia of the molecule. $T_2(\rho)$, $T_1(\rho)$, $T_0(\rho)$ and $A(\rho)$ are the functions of the bending coordinate. The bending operator derived by Hougen, Bunker, and Johns (HBJ),[17] which allows the handling of large amplitude bending vibrations, was used in this study. The last term of Eq. (2) couples two adiabatic components of the degenerate state, and, hence, the problem should be solved in a two-dimensional electronic basis. In order to avoid singularities of the Hamiltonian matrix elements, a diabatic basis, formed by the unitary transformation of the adiabatic one, was used. The matrix form of the Hamiltonian in the diabatic basis (vibronic Hamiltonian) is:

$$\begin{pmatrix} \frac{V^+ + V^-}{2} - \frac{1}{2}\left(T_1\frac{\partial^2}{\partial\rho^2} + T_2\frac{\partial}{\partial\rho} + T_0\right) + & \frac{V^+ - V^-}{2} \\ A(K^2 + \frac{C^{++} + C^{--}}{2} - 2KB^{+-}) + \Sigma B^{+-}A_{SO} & \\ \frac{V^+ - V^-}{2} & \frac{V^+ + V^-}{2} - \frac{1}{2}\left(T_1\frac{\partial^2}{\partial\rho^2} + T_2\frac{\partial}{\partial\rho} + T_0\right) + \\ & A(K^2 + \frac{C^{++} + C^{--}}{2} + 2KB^{+-}) - \Sigma B^{+-}A_{SO} \end{pmatrix} \quad (3)$$

where $V^{\pm}$ are adiabatic potentials, K is quantum number corresponding to the total orbital angular momentum. C^{++} and C^{--} are diagonal matrix elements of the square of the electronic orbital angular momentum ($\hat{L}_z^2$), and B^{+-} is the off-diagonal matrix element of $\hat{L}_z^2$.

The vibronic Schrödinger Equation was solved variationally using previously developed methods.[18–24] The vibronic wave functions were expanded in the sine basis, and all terms of the Hamiltonian (Eq. (3)) were expanded in sine or cosine bases, depending on their parity. The matrix elements of the vibronic Hamiltonian were than computed as the sums of simple trigonometric integrals, and the obtained matrix was diagonalized.

To explain the effect of spin–orbit and vibronic coupling on the ordering of the vibronic levels, another variational approach was used. All terms of the Hamiltonian were expanded in the polynomial form, and Laguerre polynomials (labeled by the two quantum numbers *v* and *l*, $|v,l\rangle$) were used as the basis for expansion of the wave function. In this case, the Bunker–Landsberg (BL) Hamiltonian was used as the kinetic energy operator for the bending vibrations. However, in the case when the bond lengths are constant, as in the present study, the BL Hamiltonian reduces to the Hougen–Bunker–Johns (HBJ) Hamiltonian.

Vibronic transition moments between the $X^2\Pi$ and $1^2\Sigma^+$ states

Perpendicular vibronic transitions between the $X^2\Pi$ and $1^2\Sigma^+$ states, which correspond to the selection rule $\Delta K = \pm 1$, are allowed within the framework of the $C_{\infty v}$ point group. When the symmetry is lowered to C_s, because of bending, parallel vibronic transitions, that correspond to the $\Delta K = 0$ selection rule, become allowed.[20] The vibronic transition intensities are proportional to the squares of the vibronic transition moments. Their forms, in the cases of parallel and perpendicular transitions, were especially derived for the present study:

$$W(K' = K'') \propto \frac{1}{2\pi}\left|\left\langle m_{\Sigma^+}\left|R_z^{++}\right|n_{\Pi^+}\right\rangle + \left\langle m_{\Sigma^+}\left|R_z^{++}\right|n_{\Pi^-}\right\rangle\right|^2$$

$$W(K' = K''+1) \propto \frac{1}{2}\frac{1}{2\pi}\left|\left\langle m_{\Sigma^+}\left|R_x^{++} - R_y^{+-}\right|n_{\Pi^+}\right\rangle + \left\langle m_{\Sigma^+}\left|R_x^{++} + R_y^{+-}\right|n_{\Pi^-}\right\rangle\right|^2 \quad (4)$$

$$W(K' = K''-1) \propto \frac{1}{2}\frac{1}{2\pi}\left|\left\langle m_{\Sigma^+}\left|R_x^{++} + R_y^{+-}\right|n_{\Pi^+}\right\rangle + \left\langle m_{\Sigma^+}\left|R_x^{++} - R_y^{+-}\right|n_{\Pi^-}\right\rangle\right|^2$$

$|n_{\Pi^\pm}\rangle$ and $|m_{\Sigma^+}\rangle$ are vibronic wave functions of the Π and Σ states, respectively, and $R^{+\pm}_{(x,y,z)}$ are the Cartesian components of the electronic transition moments between the components of the Π and Σ states. The first sign (+) in the superscript denotes the symmetry of the Σ^+ state, and the second sign (+ or –) denotes the symmetry of the component of the Π state. The molecule is placed such that the *y*-axis of the space-fixed system is perpendicular to the molecular plane at bent geometries.

The electronic transition moments were calculated as matrix elements of the dipole moment operator in the adiabatic electronic basis. The electronic wave functions were determined up to the phase factor in *ab initio* calculations, resulting in ambiguity of the sign of the computed electronic transition moments. In the case of perpendicular transitions, the values of vibronic transition moments depend on the sign of the electronic transition moments (Eq. (4)). For this reason, the correct sign of the electronic transition moments should be determined. The electronic transition moments, as electronic wave functions themselves, are monotonic functions of the molecular coordinates. Secondly, their sign at linear geometry could be determined using asymptotic dependences of the electronic functions and components of the dipole moment operator on the coordinate α (which is coordinate conjugate to the electronic angular momentum), which are of the following forms:[25]

$$\Psi^0_{\Pi^+} \propto \cos\alpha,\ \Psi^0_{\Pi^-} \propto \sin\alpha,\ \Psi^0_{\Sigma^+} \propto 1$$
$$R_{ex} \propto \cos\alpha,\ R_{ey} \propto \sin\alpha \tag{5}$$

The asymptotic values of the electronic transition moments are then:

$$R^{++}_{ex} = \left\langle \Psi_{\Sigma^+} \middle| R_{ex} \middle| \Psi_{\Pi^+} \right\rangle \propto \frac{1}{\pi}\int_0^{2\pi} \cos\alpha\ \cos\alpha d\alpha = 1$$
$$R^{+-}_{ey} = \left\langle \Psi_{\Sigma^+} \middle| R_{ey} \middle| \Psi_{\Pi^-} \right\rangle \propto \frac{1}{\pi}\int_0^{2\pi} \sin\alpha\ \sin\alpha d\alpha = 1 \tag{6}$$

Both R^{++}_{ex} and R^{+-}_{ey} have positive values at linear geometry and during bending vibrations they change such that their dependence on bending coordinate is monotonic. The dependence of *ab initio* electronic transition moments on the bending coordinate is shown in Fig. 1.

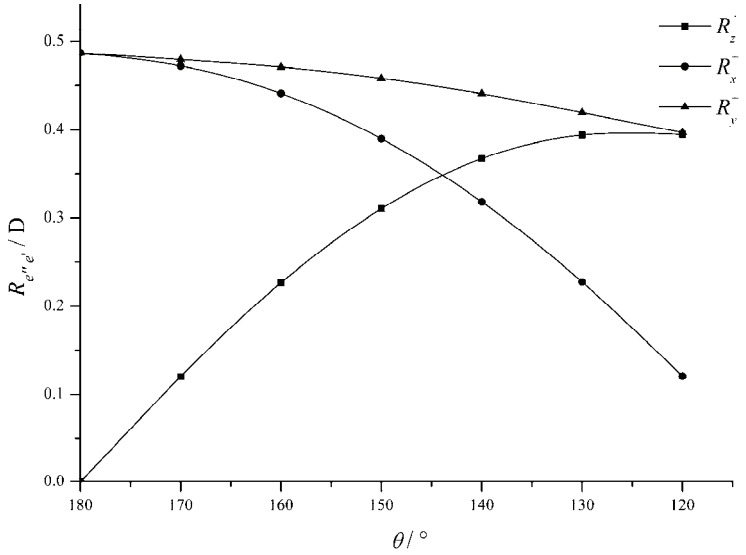

Fig. 1. MRCI bending potential energy curves of the lowest-lying doublet electronic states of HCP^+. Symmetric (A') electronic states are represented by full lines, and antisymmetric states (A'') by dashed lines.

To calculate vibronic transition moments, electronic transition moments fitted in trigonometric series and vibronic wave functions obtained by diagonalization of vibronic Hamiltonian were used. In this way, the vibronic transition moments are again represented as the sums of the simple trigonometric integrals.

RESULTS AND DISCUSSION

Electronic states

The computed MRCI bending energy curves of the lowest-lying doublet electronic states of HCP^+ are presented in Fig. 2. Degenerate electronic states are characterized by a lifting of the orbital degeneracy upon bending, *i.e.*, by the Renner–Teller (RT) effect. The $X^2\Pi$ and $1^2\Phi$ state are characterized by weak RT effects, where both state components have minima at linear geometries. The other states are examples of strong RT effects: one component of the $2^2\Pi$ and the $3^2\Pi$ state have minima at linear geometry, whereas in the cases of the $1^2\Delta$ and $2^2\Delta$ states, both of the components have minima at nonlinear geometries. In the case of a weak RT effect, the splitting of the potential energy curves upon bending in the vicinity of linear geometry follows the theoretically predicted dependence, $\rho^{2\Lambda}$, *i.e.*, the $X^2\Pi$ state shows a large splitting, whereas the splitting of the $1^2\Phi$ state is negligible.

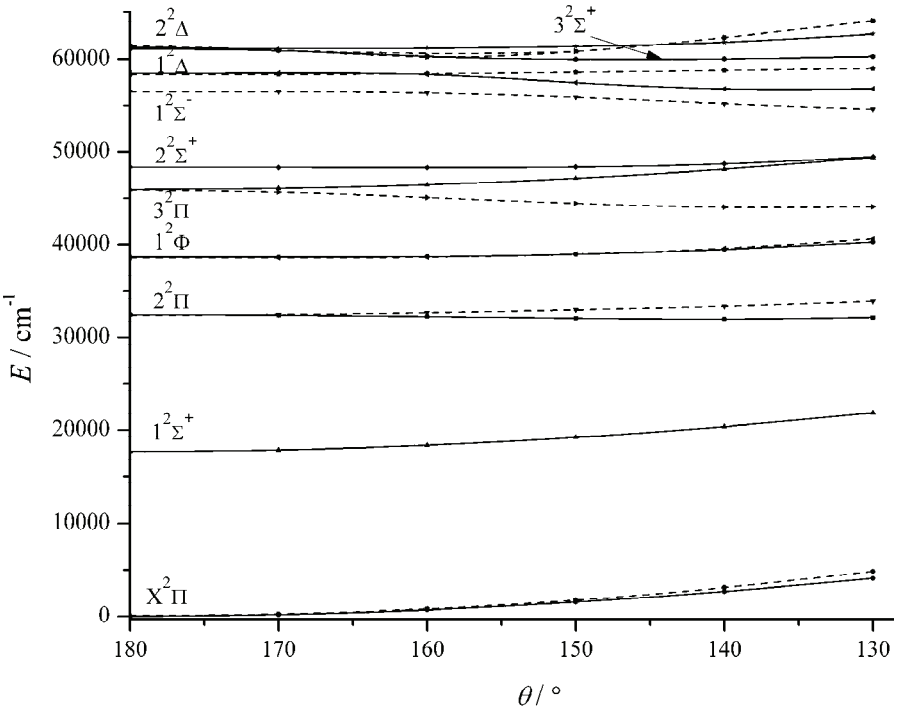

Fig. 2. Magnitudes of spin–orbit splittings of some non-unique levels in the $X^2\Pi$ state.

The electronic configuration of the $X^2\Pi$ state is $(5\sigma)^2(6\sigma)^2(7\sigma)^2(2\pi)^3$. According to the present results, the $1^2\Sigma^+$ state is formed by excitation of an electron from the 7σ to the 2π orbital, and the $2^2\Pi$, $1^2\Phi$, and $3^2\Pi$ states by excitation from the 2π to the 3π orbital. When an electron is promoted from the 7σ to the 3π orbital, three doublet states are formed, *i.e.*, $1^2\Sigma^-$, $1^2\Delta$, and $2^2\Delta$. The $7\sigma^1\ 2\pi^3\ 3\pi^1$ configuration can also give rise to quartet of states. The $2^2\Sigma^+$ and $3^2\Sigma^+$ states have more complex electronic structure - they can be approximately represented by linear combinations of three electronic configurations, $\ldots(5\sigma)^2(6\sigma)^1(7\sigma)^2(2\pi)^4$, $\ldots(5\sigma)^2(6\sigma)^2(7\sigma)^1(2\pi)^3(3\pi)^1$ and $\ldots(5\sigma)^1(6\sigma)^2(7\sigma)^2(2\pi)^4$ (Table I). Karna and Grein[9] found that the configurations obtained by excitation of an electron from the 7σ to the 4π orbital contribute significantly to some excited states ($2^2\Pi$, $1^2\Delta$ and $1^2\Sigma^-$). The present calculations were performed such that 4π orbital was also a part of the active space, but the configuration state functions in which it was occupied by an electron gave negligible contributions to the wave functions of the mentioned states. Differences in the electronic configurations explain the significant discrepancies in the vertical excitation energies in cases of the $2^2\Pi$ and $1^2\Sigma^-$ states (Table I). Unfortunately, no experimental results are available for these states. The calculated excitation energies of the other excited states are in plausible accordance with the available theoretical results.

TABLE I. Electronic configurations of the ten lowest-lying doublet electronic states of HCP^+, vertical excitation energies, electronic transition moments and oscillator strengths for transitions from the ground $X^2\Pi$ state to the corresponding excited states

State ($C_{\infty v}$)	Dominant configurations	T_e / cm^{-1}	$\lvert R_{e''e'}\rvert$ / D	f
$X^2\Pi$	$\ldots(5\sigma)^2(6\sigma)^2(7\sigma)^2(2\pi)^3$	0.00	1.545209 (z)	–
$1^2\Sigma^+$	$\ldots(5\sigma)^2(6\sigma)^2(7\sigma)^1(2\pi)^4$	17507[b]	0.464382 (x,y)	0.0071
		18067		
		16776		
$2^2\Pi$	$\ldots(5\sigma)^2(6\sigma)^2(7\sigma)^2(2\pi)^2(3\pi)^1$	32159	0.623049 (z)	0.0236
		26939		
$1^2\Phi$	$\ldots(5\sigma)^2(6\sigma)^2(7\sigma)^2(2\pi)^2(3\pi)^1$	38508	Forbidden	
$3^2\Pi$	$\ldots(5\sigma)^2(6\sigma)^2(7\sigma)^2(2\pi)^2(3\pi)^1$	45769	0.358802 (z)	0.0028
$2^2\Sigma^+$	$c_1\lvert\Psi_1\rangle + c_2\lvert\Psi_2\rangle + c_3\lvert\Psi_3\rangle$ [a]	48120	0.487279 (x,y)	0.0215
		49119		
$1^2\Sigma^-$	$\ldots(5\sigma)^2(6\sigma)^2\ (7\sigma)^1(2\pi)^3(3\pi)^1$	57414	0.482024 (x,y)	0.0251
		60572		
$1^2\Delta$	$\ldots(5\sigma)^2(6\sigma)^2\ (7\sigma)^1(2\pi)^3(3\pi)^1$	58244	0.700384 (x,y)	0.2149
		57669		
$3^3\Sigma^+$	$c_1'\lvert\Psi_1\rangle + c_2'\lvert\Psi_2\rangle + c_3'\lvert\Psi_3\rangle$ [a]	60849	0.592387 (x,y)	0.0402
$2^2\Delta$	$\ldots(5\sigma)^2(6\sigma)^2\ (7\sigma)^1(2\pi)^3(3\pi)^1$	61129	1.054598 (x,y)	0.5115

[a]The vectors $\lvert\Psi_1\rangle$,$\lvert\Psi_2\rangle$ and $\lvert\Psi_3\rangle$ denote the electronic configurations $(5\sigma)^2(6\sigma)^1(7\sigma)^2(2\pi)^4$, $(5\sigma)^2(6\sigma)^2(7\sigma)^2(2\pi)^3$ and $(5\sigma)^1(6\sigma)^2(7\sigma)^2(2\pi)^4$, respectively; [b]The first values of T_e in the cells were obtained in this study, the second values (where available) are theoretical values obtained by Karna and Grein[9] and the third result for the $1^2\Sigma^+$ state is an experimental value

In order to inspect the character of the excited states, the vertical ionization energy from the ground state of the HCP^+ ion to the $X^1\Sigma^+$ state of the HCP^{2+} was computed. It is found that the vertical ionization energy, expressed in wave numbers, was IP_ν = 156800 cm^{-1}. The energetic terms of the Rydberg states can be calculated by application of the Rydberg Formula, $T_n = IP - R / (n - \Delta)^2$,[26] where IP is the ionization energy, R is the Rydberg constant, n is the principal quantum number, and Δ is the quantum defect of the state in question. It could be estimated that the lowest-lying Rydberg states (for $n - \Delta = 1$) of the HCP^+ could be expected at approximately 47000 cm^{-1} above the minimum of the ground state. There is a possibility that the $2^2\Sigma^+$, $1^2\Sigma^-$, $1^2\Delta$, $3^2\Sigma^+$ and $2^2\Delta$ states are Rydberg states because their vertical excitation energies surpass the given value. In order to inspect this, calculations of the vertical excitation energies were performed with aug-cc-pVTZ basis sets augmented by one set of diffuse *s* and *p* orbitals built in an even tempered manner from the exponents of the two most diffuse *s* and *p* functions[27] (exponents of additional diffuse functions are: hydrogen *s* (0.006212) and *p* (0.026815); carbon *s* (0.015080) and *p* (0.0101536); phosphorous *s* (0.015856) and *p* (0.009702)). The excitation energies of all the studied states obtained with the augmented set differed negligibly from those obtained with aug-cc-pVTZ set. Hence, it was concluded that the studied electronic states do not have marked Rydberg character.

By inspecting the calculated values of the electronic transition moments at linear geometry (Table I), it could be concluded that the most probable are transitions to the $1^2\Delta$ and $2^2\Delta$ states. The transition moments to other states are of smaller magnitude.

The dimensionless quantity that expresses the strength of the transition between two quantum states, oscillator strength, is defined as:

$$f_{12} = \frac{2}{3}(E_2 - E_1)\sum_{m_2}\sum_{\alpha=\mathrm{x,y,z}}\left|\langle 1m_1|R_\alpha|2m_2\rangle\right|^2 \qquad (7)$$

where E_1 and E_2 are the energies of the $|1m_1\rangle$ and $|2m_2\rangle$ quantum states, which can have several degenerate sub-states labeled by m_1 and m_2. R_α are the Cartesian components of the electronic transition operator between states. All quantities in Eq. (7) are expressed in atomic units. The calculated values of the oscillator strengths for transitions between the ground and studied excited states are presented Table I. The most intensive transitions to $2^2\Delta$ and $1^2\Delta$ are expected. The oscillator strengths for other transitions are at least one order of magnitude smaller.

Vibronic structure of the $X^2\Pi$ state

The bending potential curves of the X^2A' and $1^2A''$ components of the $X^2\Pi$ state are fitted in a polynomial form as the functions of the coordinate ρ:

$$E(X\,^2A') = 0.026135\rho^2 - 0.002018\rho^4$$
$$E(1^2A'') = 0.027678\rho^2 - 0.001252\rho^4 \quad (8)$$

where the energies are expressed in hartrees and the angles in radians.

The most important molecular parameters of the $X^2\Pi$ state obtained in this study using *ab initio* methods and the available experimental and theoretical values are given in Table II. The calculated parameters are compared with the corresponding experimental values.

TABLE II. Molecular parameters of HCP^+ in the $X^2\Pi$ state

Parameter	MRCI/CASSCF/ aug-cc-pVTZ (this work)	Emission spectrum study[3,4]	LIF spectrum study[5a]
r_{HC} / Å	1.0839	1.11(4)	1.077(2)
r_{CP} / Å	1.6129	1.596(5)	1.6013(3)
ω_1 / cm^{-1}	3144	–	2986.0 (3124.8)
ω_2 / cm^{-1}	639	–	717.5 (642.7)
ω_3 / cm^{-1}	1277	1150.0	1282.0 (1156.0)
A_{SO} / cm^{-1}	–129.3	–146.97	–148.4
ε	–0.0313	–	(–0.034(2))
$\varepsilon\omega_2$/ cm^{-1}	–20.0	–26.(4)	–22.0

The $X^2\Pi$ state is characterized by a relatively large value of the spin–orbit coupling constant (A_{SO} = –148.4 cm^{-1}), which is approximately seven times larger than the product of the Renner parameter and the bending frequency ($\varepsilon\omega_2$ = = 22 cm^{-1}). According to this, it would be expected that the spin–orbit interaction determines the ordering of the vibronic levels.

The computed bending vibronic levels up to ≈2500 cm^{-1} of Σ (K = 0), Π (K = 1), Δ (K = 2), and Φ (K = 3) symmetries of the $X^2\Pi$ electronic states, the available experimental values and the compositions of the vibronic wave functions in terms of Laguerre polynomials are given in Table III. The theoretical values obtained variationally by Biczysko and Tarroni[11] are also given. They were able to reproduce satisfactorily the energies, but the order of some levels was different from the experimental assignment. For example, this was the case with the close-lying $(0,2,0)\mu\Pi_{3/2}$ and $(0,2,0)\mu\Pi_{1/2}$ levels. Only the results obtained with the first described variational method (with expansions in trigonometric basis) are presented. They are in satisfactory agreement with experimental and theoretical results. The second method based on the expansion in Laguerre polynomials gives excellent results for the low-lying vibronic levels, but significant deviations from the available experimental values occur for the higher levels. The second method is here used to obtain the approximate compositions of the vibronic wave functions in terms of Laguerre polynomials.

The magnitude of the spin–orbit splittings of the unique levels (represented with one Laguerre polynomial) is equal to the spin–orbit constant (for example,

$(0,0,0)\Pi_{3/2}$ and $(0,0,0)\Pi_{1/2}$, $(0,1,0)\Delta_{3/2}$ and $(0,1,0)\Delta_{5/2}$). On the other hand, the obtained spin components of the non-unique levels, which are approximately described as linear combinations of two Laguerre polynomials, are very close to each other. In the absence of spin–orbit coupling, the contribution of both polynomials is approximately equal. When spin–orbit coupling is taken into account, the contribution of one Laguerre polynomial becomes dominant and of the other one much smaller, because relatively strong spin–orbit interaction "tends" to decouple relatively weakly coupled vibronic levels. The signs of the expansion coefficients are such that when one vibronic level is combined with $\Sigma = 1/2$ or $\Sigma = -1/2$, the energies of both obtained spin components are shifted in the same direction compared to the case when spin–orbit interaction is not taken into account (Fig. 3). For this reason, the obtained spin components are very similar in energies in some cases and the magnitude of their splitting depends on the strength of the vibronic coupling. Hence, the level of sophistication in treatment of kinetic energy and anharmonic resonances can significantly influence the structure of the spectrum.

TABLE III. Energies obtained in this study for the lowest vibronic levels in the $X^2\Pi$ state, and the available theoretical and experimental values

Level	Composition	E / cm^{-1}		
		Calculated (this work)	Experimental[4]	Calculated[11]
$(0,0,0)\Pi_{3/2}$	$\|0,0\rangle$ (u)	0.0	0.0	0.0
$(0,0,0)\Pi_{1/2}$	$\|0,0\rangle$ (u)	148.3	148.1	148.2
$(0,1,0)\mu\Sigma^+$	$0.986\|1,1\rangle + 0.163\|1,-1\rangle$	632.6	633.4	631.6
$(0,1,0)\Delta_{5/2}$	$\|1,1\rangle$ (u)	636.8	648.3	642.6
$(0,1,0)\kappa\Sigma^-$	$-0.162\|1,1\rangle + 0.986\|1,-1\rangle$	790.4	786.5	787.0
$(0,1,0)\Delta_{3/2}$	$\|1,1\rangle$ (u)	785.1	796.0	790.1
$(0,2,0)\mu\Pi_{3/2}$	$0.975\|2,0\rangle - 0.219\|2,2\rangle$	1240.8	1260.9	1257.3
$(0,2,0)\mu\Pi_{1/2}$	$-0.282\|2,0\rangle + 0.959\|2,2\rangle$	1262.1	1256.0	1259.2
$(0,2,0)\Phi_{7/2}$	$\|2,2\rangle$ (u)	1271.5		1290.9
$(0,2,0)\kappa\Pi_{1/2}$	$0.958\|2,0\rangle + 0.280\|2,2\rangle$	1408.4	1426.8	1418.8
$(0,2,0)\Phi_{5/2}$	$\|2,2\rangle$ (u)	1420.0		1437.5
$(0,2,0)\kappa\Pi_{3/2}$	$0.217\|2,0\rangle - 0.975\|2,2\rangle$	1429.8		1433.5
$(0,3,0)\mu\Sigma^+$	$0.937\|2,0\rangle - 0.348\|4,2\rangle$	1868.7		1871.8
$(0,3,0)\mu\ \Delta_{3/2}$	$-0.404\|3,1\rangle + 0.915\|3,3\rangle$	1909.3		1887.3
$(0,3,0)\mu\ \Delta_{5/2}$	$0.966\|3,1\rangle - 0.254\|3,3\rangle$	1875.3	1896.1	1889.2
$(0,3,0)\kappa\Sigma^-$	$-0.345\|2,0\rangle + 0.935\|4,2\rangle$	2056.1		2053.7
$(0,3,0)\kappa\ \Delta_{3/2}$	$0.912\|3,1\rangle + 0.401\|3,3\rangle$	2055.3		2058.1
$(0,3,0)\kappa\ \Delta_{5/2}$	$0.251\|3,1\rangle + 0.966\|3,3\rangle$	2089.5		2086.9
$(0,4,0)\mu\Pi_{3/2}$	$0.923\|4,0\rangle - 0.383\|4,2\rangle$	2494.8		2490.9
$(0,4,0)\mu\Pi_{1/2}$	$-0.459\|4,0\rangle + 0.888\|4,2\rangle$	2509.6	2492.5	2492.3

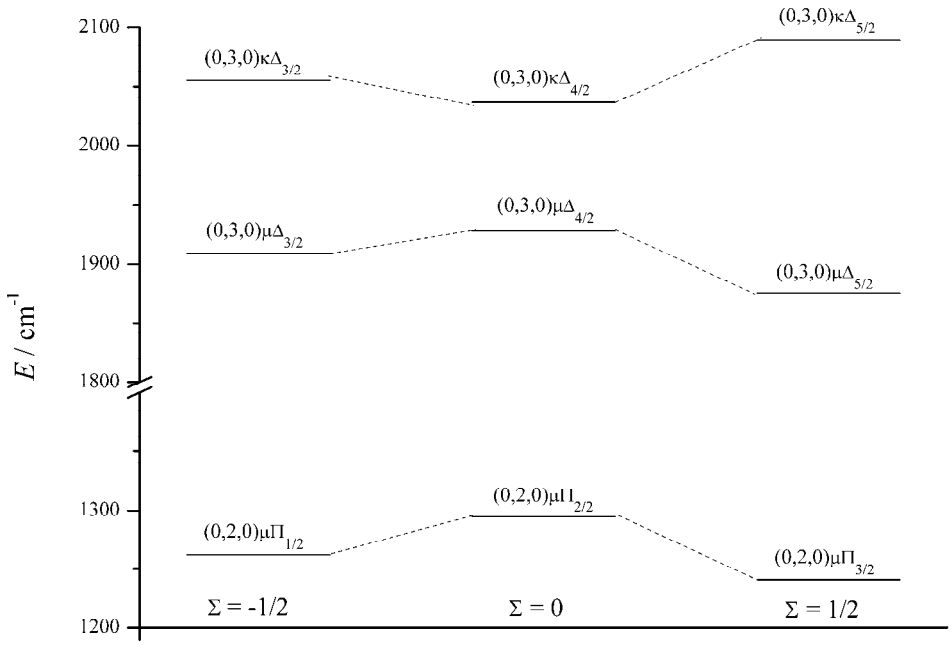

Fig. 3. Dependence of the electronic transition moments between the $X^2\Pi$ and $1^2\Sigma^+$ states on the bending coordinate.

Vibronic transitions between the $X^2\Pi$ and $1^2\Sigma^+$ states

The squared values of the vibronic transition moments between low-lying vibronic levels of the $X^2\Pi$ and $1^2\Sigma^+$ states are given in Table IV. According to the results, vibronic transitions corresponding to the $\Delta K = 0$ selection rule are of low intensity. The reason for this is that the *z*-component of the electronic transition moment, which induces these transitions, is zero at linear geometry and becomes large only when molecule is significantly bent.

On the other hand, several intensive perpendicular transitions ($\Delta K = \pm 1$) occur. The most intensive ones arise from unique levels of the $X^2\Pi$ state, particularly from the lowest unique $K'' = 1$ level, $|0,0\rangle$ to the lowest $K' = 1$ level of the $1^2\Sigma^+$ state, which is also described by a $|0,0\rangle$ polynomial. Also, the transition between unique $K'' = 2$ $|1,1\rangle$ level to the $|1,1\rangle$ level of the $1^2\Sigma^+$ state is intensive. Several intensive transitions from non-unique levels of the $X^2\Pi$ state composed predominantly of one Laguerre polynomial to vibronic levels of the $1^2\Sigma^+$ state described by the same Laguerre polynomial exist. For example, the transition between the first $K'' = 0$ level, which is approximately described as $-0.163|1,-1\rangle + 0.986|1,1\rangle$ and the first K' = 1 level composed of $|1,1\rangle$ polynomial is intensive.

TABLE IV. Squared vibronic transition moments in D^2 between the vibronic levels of the $X^2\Pi$ and $1^2\Sigma^+$ states for the case $\Sigma = -1/2$. The vibronic levels of the $X^2\Pi$ state are placed vertically and the levels of the $1^2\Sigma^+$ state are placed horizontally. The compositions of the vibronic levels in terms of Laguerre polynomials are given for each level

$K''=0$	$K'=0$				
	$\|0,0\rangle$	$\|2,0\rangle$	$\|4,0\rangle$	$\|6,0\rangle$	$\|8,0\rangle$
$0.163\|1,-1\rangle+0.986\|1,1\rangle$	0.709–2	0.629–2	0.189–4	0.871–6	0.166–5
$0.986\|1,-1\rangle-0.162\|1,1\rangle$	0.165–1	0.145–1	0.521–4	0.204–5	0.377–5
$0.348\|3,-1\rangle+0.937\|3,1\rangle$	0.145–4	0.771–2	0.612–2	0.237–4	0.233–5
$0.935\|3,-1\rangle-0.345\|3,1\rangle$	0.735–4	0.322–1	0.250–1	0.148–3	0.873–5
$0.483\|5,-1\rangle+0.875\|5,1\rangle$	0.708–6	0.696–5	0.420–2	0.378–2	0.180–5
$K''=1$	$K'=0$				
	$\|0,0\rangle$	$\|2,0\rangle$	$\|4,0\rangle$	$\|6,0\rangle$	$\|8,0\rangle$
$\|0,0\rangle$	0.225+0	0.116–6	0.450–5	0.306–6	0.281–7
$-0.282\|2,0\rangle+0.959\|2,2\rangle$	0.834–4	0.217–1	0.104–3	0.558–6	0.152–4
$0.958\|2,0\rangle+0.280\|2,2\rangle$	0.961–3	0.180+0	0.340–3	0.399–5	0.451–6
$-0.459\|4,0\rangle+0.888\|4,2\rangle$	0.803–4	0.360–3	0.492–1	0.806–3	0.122–3
$0.884\|4,0\rangle+0.454\|4,2\rangle$	0.270–4	0.736–3	0.134+0	0.318–3	0.574–4
$K''=1$	$K'=2$				
	$\|2,2\rangle$	$\|4,2\rangle$	$\|6,2\rangle$	$\|8,2\rangle$	$\|10,2\rangle$
$\|0,0\rangle$	0.488–3	0.656–4	0.994–4	0.873–4	0.491–3
$-0.282\|2,0\rangle+0.959\|2,2\rangle$	0.173+0	0.109–2	0.948–4	0.173–4	0.334–1
$0.958\|2,0\rangle+0.280\|2,2\rangle$	0.214–1	0.425–3	0.200–4	0.286–4	0.152–2
$-0.459\|4,0\rangle+0.888\|4,2\rangle$	0.177–2	0.142+0	0.128–2	0.197–4	0.704–4
$0.884\|4,0\rangle+0.454\|4,2\rangle$	0.141–1	0.983–2	0.476–1	0.626–4	0.700–5
$K''=0$	$K'=1$				
	$\|1,1\rangle$	$\|3,1\rangle$	$\|5,1\rangle$	$\|7,1\rangle$	$\|9,1\rangle$
$0.163\|1,-1\rangle+0.986\|1,1\rangle$	0.120+0	0.702–1	0.892–2	0.165–2	0.346–3
$0.986\|1,-1\rangle-0.162\|1,1\rangle$	0.544–2	0.614–3	0.249–3	0.113–5	0.231–6
$0.986\|1,-1\rangle-0.162\|1,1\rangle$	0.306–1	0.822–1	0.560–1	0.616–2	0.238–2
$0.935\|3,-1\rangle-0.345\|3,1\rangle$	0.569–2	0.941–2	0.962–3	0.124–2	0.403–4
$0.483\|5,-1\rangle+0.875\|5,1\rangle$	0.142–1	0.112–1	0.588–1	0.576–1	0.164–2
$K''=1$	$K'=1$				
	$\|1,1\rangle$	$\|3,1\rangle$	$\|5,1\rangle$	$\|7,1\rangle$	$\|9,1\rangle$
$\|0,0\rangle$	0.778–2	0.364–2	0.544–3	0.713–4	0.819–5
$-0.282\|2,0\rangle+0.959\|2,2\rangle$	0.524–2	0.120–1	0.366–7	0.159–5	0.750–8
$0.958\|2,0\rangle+0.280\|2,2\rangle$	0.155–2	0.397–1	0.214–2	0.464–3	0.143–3
$-0.459\|4,0\rangle+0.888\|4,2\rangle$	0.883–3	0.265–2	0.687–2	0.459–5	0.275–4
$0.884\|4,0\rangle+0.454\|4,2\rangle$	0.243–3	0.669–2	0.622–1	0.320–2	0.156–3
$K''=2$	$K'=1$				
	$\|1,1\rangle$	$\|3,1\rangle$	$\|5,1\rangle$	$\|7,1\rangle$	$\|9,1\rangle$
$\|1,1\rangle$	0.125+0	0.705–1	0.914–2	0.166–2	0.334–3
$-0.404\|3,1\rangle+0.915\|3,3\rangle$	0.488–2	0.157–1	0.114–1	0.498–3	0.398–3
$0.912\|3,1\rangle+0.401\|3,3\rangle$	0.309–1	0.756–1	0.448–1	0.684–2	0.198–2
$-0.550\|5,1\rangle+0.834\|5,3\rangle$	0.642–2	0.554–2	0.276–1	0.282–1	0.155–3
$0.828\|5,1\rangle+0.543\|5,3\rangle$	0.141–1	0.983–2	0.476–1	0.307–1	0.369–2

In conclusion, all intensive vibronic transitions between the $X^2\Pi$ and $1^2\Sigma^+$ states correspond to the selection rules $\Delta K = \pm 1$ and $\Delta v = 0$. They occur between levels whose wave functions overlap significantly, which is the case between unique levels of the $X^2\Pi$ state or non-unique levels of similar composition as the unique ones and vibrational levels of the $1^2\Sigma^+$ state composed of the same Laguerre polynomial.

CONCLUSIONS

The low-lying doublet excited states of HCP^+ were studied by means of the internally contracted MRCI method. The computed bending potentials of the $X^2\Pi$ state were employed in variational calculations of the vibronic energy levels using the model Hamiltonian that neglects coupling between stretching and bending modes. The applied method gave results for the vibronic levels that were in accordance with the experimental values up to 2500 cm^{-1}. The obtained wave functions were utilized for the calculation of the vibronic transition moments between the $X^2\Pi$ and $1^2\Sigma^+$ states. According to the results, the most intensive are perpendicular transitions with the selection rule $\Delta v = 0$ between unique levels of the $X^2\Pi$ state or non-unique levels of similar composition as the unique ones and vibrational levels of the $1^2\Sigma^+$ state.

Acknowledgments. The author gratefully acknowledges Professor Fiedrich Grein for sending a copy of his paper on the HCP^+ and Professor Miljenko Perić for support and for allowing the use of his programs for solving the vibronic Schrödinger Equation. This study was financially supported by the Ministry of Education, Science and Technological Development of the Republic of Serbia (Project No. 172040).

ИЗВОД

АВ INITIO ПРОУЧАВАЊЕ ВИБРОНСКИХ ПРЕЛАЗА ИЗМЕЂУ $X^2\Pi$ И $1^2\Sigma^+$ СТАЊА HCP^+

ЉИЉАНА СТОЈАНОВИЋ

Факултет за физичку хемију, Универзитет у Београду, Студентски трг 12, 11158 Београд

Дублетна нисколежећа електронска стања HCP^+ су проучавана помоћу методе мултиреферентне интеракције конфигурација. Енергије вибронских нивоа $X^2\Pi$ стања Σ, Π, Δ, и Φ симетрија до 2500 cm^{-1} су израчунате применом варијационих метода које узимају у обзир вибронску и спин–орбитну интеракцију. Израчунате вибронске таласне функције су искоришћене у прорачунима момената прелаза између вибронских нивоа $X^2\Pi$ и $1^2\Sigma^+$ електронских стања. Добијене вредности су упоређене са доступним експерименталним и теоријским резултатима.

(Примљено 15. новембра, ревидирано 25. новембра 2012)

REFERENCES

1. D. C. Frost, S. T. Lee, C. A. McDowell, *Chem. Phys. Lett.* **23** (1973) 472
2. M. A. King, H. W. Kroto, J. F. Nixon, D. Klapstein, J. P. Maier, O. Marthaler, *Chem. Phys. Lett.* **82** (1981) 543

3. M. A. King, D. Klapstein, H. W. Kroto, J. P. Maier, J. F. Nixon, *J. Mol. Struct.* **80** (1982) 23
4. M. A. King, R. Kuhn, J. P. Mayer, *Mol. Phys.* **60** (1987) 867
5. F. X. Sunahori, X. Zhang, D. J. Clouthier, *J. Chem. Phys.* **127** (2007) 104312
6. F. T. Chau, Y. W. Tang, X. Song, *J. Mol. Struct. (THEO-CHEM)* **280** (1993) 233
7. P. J. Bruna, G. Hirsch, R. J. Buenker, S. D. Peyerimhoff, in *Molecular Ions: Geometric and Electronic Structures*, NATO ASI Ser. B, vol. 90, J. Berkowitz and K.-O. Groeneveld, Eds., Plenum Press, New York, 1983, p. 309
8. P. Botschwina, P. Sebald, *J. Mol. Spectrosc*., **100** (1983) 1
9. S. P. Karna, F. Grein, *Chem. Phys. Lett.* **169** (1990) 161
10. B. Temelso, N. A. Richarson, L. Sari, Y. Yamaguchi, H. F. Schaefer, *J. Theor. Comput. Chem.* **4** (2005) 707
11. M. Biczysko, R. Tarroni, *Phys. Chem. Chem. Phys.* **4** (2002) 708
12. a) H.-J. Werner, P. J. Knowles, *J. Chem. Phys.* **89** (1988) 5803; b) P. J. Knowles, H.-J. Werner, *Theor. Chim. Acta* **84** (1992) 95
13. a) H.-J. Werner, P. J. Knowles, *J. Chem. Phys.* **82** (1985) 5053; b) P. J. Knowles, H.-J. Werner, *Chem. Phys. Lett.* **115** (1985) 259
14. T. H. Dunning, Jr., *J. Chem. Phys.* **90** (1989) 1007
15. MOLPRO, a package of *ab initio* programs designed by H.-J. Werner and P. J. Knowles, version 2006.1, http://www.molpro.net
16. M. Perić, S. D. Peyerimhoff, in *The Role of Degenerate States in Chemistry*, *Advances in Chemical Physics*, Vol. 124, M. Baer, G. D. Billing, Eds., Wiley, New York, 2002, p. 583
17. J. T. Hougen, P. R. Bunker, J. W. C. Johns, *J. Mol. Spectrosc.* **34** (1970) 136
18. M. Perić, S. D. Peyerimhoff, R. J. Buenker, *Mol. Phys.* **49** (1983) 379
19. M. Perić, S. D. Peyerimhoff, R. J. Buenker, *Int. Rev. Phys. Chem.* **4** (1985) 85
20. M. Perić, R. J. Buenker, S. D. Peyerimhoff, *Mol. Phys.* **59** (1986) 1283
21. M. Perić, B. Ostojić, J. Radić-Perić, *Phys. Rep.* **290** (1997) 283
22. S. Jerosimić, Lj. Stojanović, M. Perić, *J. Chem. Phys.* **133** (2010) 024307
23. M. Perić, B. Engels, S. D. Peyerimhoff, in *Quantum Mechanical Electronic Structure Calculations with Chemical Accuracy*, S. R. Langhoff, Ed., Kluwer, Dordrecht, 1995, p. 261
24. S. Jerosimić, M. Perić, *J. Chem. Phys.* **129** (2008) 144305
25. Lj. Stojanović, S. Jerosimić, M. Perić, *Chem. Phys.* **379** (2011) 57
26. M. Perić, S. D. Peyerimhoff, in *The Role of Rydberg States in Spectroscopy and Photochemistry*, C. Sándorfy, Ed., Kluwer, Dordrecht, The Netherlands, 1999, p. 137
27. R. Vetter, T. Ritschel, L. Zülicke, K. Peterson, *J. Phys. Chem., A* **107** (2003) 1405.